

Centrifugal Microfluidics with Integrated Sensing Microdome Optodes for Multiion Detection

Amanda S. Watts,[†] Aaron A. Urbas,[†] Elissavet Moschou,[†] Vasilis G. Gavalas,[†] Jim V. Zoval,[‡] Marc Madou,[‡] and Leonidas G. Bachas^{*,†}

Department of Mechanical and Aerospace Engineering, University of California, Irvine, California 92697, Department of Chemistry, University of Kentucky, Lexington, Kentucky 40506-0055

An array of four sensing microdome optodes (potassium, sodium, calcium, and chloride) was incorporated into a centrifugal microfluidics platform to obtain a multiion analysis system. The behavior of each sensing microdome was in good agreement with a theoretical model describing the response. The selectivity of each optode over common interfering ions was established and was used to identify calibrant solutions that can be employed for the simultaneous calibration of all four optodes without significant cross-interference. The microfluidic platform was designed to facilitate both three-point calibration of the optodes and triplicate analysis of a sample within a single run, which increases the accuracy of the determination. The optimized microfluidic system was used to determine simultaneously the concentration of potassium, sodium, calcium, and chloride in aquarium water (with the composition of Lake Tanganyika water) with less than 6% error. The simple process of fabrication of these microdomes and their incorporation into a centrifugal microfluidic platform should facilitate the development of portable ion-sensing analysis systems.

Extended scientific research in the area of micro total analysis systems (μ TAS) has occurred since their inception in the early 1990s.^{1,2} With the recent advances in miniaturization, integrated devices which can perform various analytical functions have been developed and have been termed labs-on-a-chip.³ These systems have many advantages, such as low power and space requirements, as well as the need for very small amounts of sample and reagent. For instance, in the healthcare industry, these integrated systems could provide high-throughput analysis and automation and reduce sample volume and reagent consumption significantly.⁴

To date, few microfluidic systems have been developed for ion detection. One commercially available system is the i-STAT clinical analyzer, which is composed of a portable hand-held analyzer and

disposable cartridges.^{5–7} Detection of ions is accomplished inside the cartridges by an array of thin-film microelectrodes, or biosensors, microfabricated on a silicon chip. The calibrant solution, a sample-handling system, and conductivity pads for electrical contact with the analyzer are also contained within the cartridges. While this system demonstrated reproducible results and ease of use, a drawback is the one-point calibration performed prior to sample analysis. Tantra and Manz introduced a potentiometric chip-based sensor employing ion-selective electrodes capable of detecting barium in the range of 10^{-1} – 10^{-6} M.⁸ Recently, potassium- and sodium-sensing has been accomplished on microfluidic chips by employing ionophore-based ion pair extraction.^{9,10} Capillary-assembled microchips, which consist of chemically functionalized square capillaries embedded into a poly-(dimethylsiloxane) (PDMS) microchannel network, were introduced by Hisamoto and co-workers for calcium- and pH-sensing.¹¹ The incorporation of multiple ion-sensing capillaries into the PDMS lattice enabled the detection of potassium, sodium, and calcium.¹² Continuous-flow chemical processing was developed by Kitamori and co-workers for cobalt(II) determination.¹³ This technique involved the integration of a multiphase flow network and several microunit operations, including mixing and reaction, two and three-phase fluid flow, and solvent extraction.

Centrifugal microfluidics propulsion devices consist of a disc-shaped substrate containing microfabricated microfluidics architectures of channels and reservoirs. Flow is accomplished in centrifugal microfluidics systems through the radial forces that develop from the spinning of the disc-shaped platform and depends on factors such as angular frequency of rotation, fluid properties such as viscosity and density, and the dimensions and

* Corresponding author. E-mail: bachas@uky.edu. Phone: (859)257-6350. Fax: (859)323-1069.

[†] University of Kentucky.

[‡] University of California.

(1) Kutter, J. P. *TrAC, Trends Anal. Chem.* **2000**, *19*, 352–363.

(2) Reyes, D. R.; Iossifidis, D.; Auroux, P.-A.; Manz, A. *Anal. Chem.* **2002**, *74*, 2623–2636.

(3) Weigl, B. H.; Yager, P. *Science* **1999**, *283*, 346–347.

(4) Figeys, D.; Pinto, D. *Anal. Chem.* **2000**, *72*, 330A–335A.

(5) Erickson, K. A.; Wilding, P. *Clin. Chem.* **1993**, *39*, 283–287.

(6) Jacobs, E.; Vadasdi, E.; Sarkozi, L.; Coman, N. *Clin. Chem.* **1993**, *39*, 1069–1074.

(7) Mock, T.; Morrison, D.; Yatscoff, R. *Clin. Biochem.* **1995**, *28*, 187–192.

(8) Tantra, R.; Manz, A. *Anal. Chem.* **2000**, *72*, 2875–2878.

(9) Hisamoto, H.; Horiuchi, T.; Tokeshi, M.; Hibara, A.; Kitamori, T. *Anal. Chem.* **2001**, *73*, 1382–1386.

(10) Hisamoto, H.; Horiuchi, T.; Uchiyama, K.; Tokeshi, M.; Hibara, A.; Kitamori, T. *Anal. Chem.* **2001**, *73*, 5551–5556.

(11) Hisamoto, H.; Nakashima, Y.; Kitamura, C.; Funano, S.; Yasuoka, M.; Morishima, K.; Kikutani, Y.; Kitamori, T.; Terabe, S. *Anal. Chem.* **2004**, *76*, 3222–3228.

(12) Hisamoto, H.; Yasuoka, M.; Terabe, S. *Anal. Chim. Acta* **2006**, *556*, 164–170.

(13) Tokeshi, M.; Minagawa, T.; Uchiyama, K.; Hibara, A.; Sato, K.; Hisamoto, H.; Kitamori, T. *Anal. Chem.* **2002**, *74*, 1565–1571.

locations of the channels.¹⁴ Centrifugal propulsion is a potential alternative to other pumping methods most commonly employed in μ TAS applications, including syringe or peristaltic pumping, and electroosmotic flow. Because only a motor is needed to spin the platform, a system operating by this method is safer and has lower power and space requirements. Whereas electroosmotic pumping is affected by the pH and ionic strength of the liquid, these parameters have no influence on centrifugal pumping. Using this pumping technique, Duffy and co-workers successfully pumped the biological fluids blood and urine, as well as a buffer containing a detergent used in the polymerase chain reaction and the organic solvent dimethyl sulfoxide.¹⁵ Trapped air bubbles do not present a problem, because centrifugal pumping dispels them. Additionally, there is no limitation on channel size or flow rate.¹⁵ The theory of centrifugal propulsion on microfluidic discs has been discussed previously in detail.^{15,16}

Fully integrated μ TAS have been reported that incorporate ion-selective optodes for potassium^{17,18} or nitrite-sensing¹⁸ on a centrifugal microfluidics platform. In this system, the optode membrane was spin-coated onto the nonadhesive side of a piece of tape and then placed over the detection chamber on the microfluidic disc. This design is not easily amenable to multiion sensing using an array of different optodes within the same microfluidic network. To facilitate multiion sensing, in our present study we integrate a novel ion-sensing optode architecture with centrifugal microfluidics. The microfluidics platform was designed to contain six solution reservoirs, and the sensing components were miniaturized by placing an array of microspotted domed-shaped optodes in the detection chamber to enable multianalyte detection. A versatile microspotting on silanized glass approach was adapted that could allow for parallel manufacturing of microdome optode arrays. More importantly, the formulation of the optodes and calibrating solutions was optimized so that four different ion optodes could be calibrated simultaneously using three multiion containing solutions with minimal cross-interference to yield a set of four three-point calibration plots.

EXPERIMENTAL SECTION

Materials. Bis(2-ethylhexyl) sebacate, 9-(diethylamino)-5-(2-octadecylimino)benzo[a]phenoxazine (Chromoionophore III, ETH 5350), 4',5'-dibromofluorescein octadecyl ester (Chromoionophore VI, ETH 7075), 4-*tert*-butylcalix[4]arene-tetraacetic acid tetraethyl ester (sodium ionophore X), *N,N,N',N'*-tetracyclohexyl-3-oxapentanediamide (calcium ionophore II, ETH 129), tridodecylmethylammonium chloride (TDMAC), sodium tetrakis[3,5-bis-(trifluoromethyl)phenyl]borate (NaTFPB), and potassium tetrakis[3,5-bis-(trifluoromethyl)phenyl]borate (KTFPB) were obtained from Fluka (Milwaukee, WI). Benzoyl peroxide, benzophenone, 3-(trimethoxysilyl)propyl methacrylate (MPTS), and 1,6-hexanediol dimethacrylate (HDDMA) were purchased from Sigma-Aldrich (St. Louis, MO). Valinomycin was obtained from Acros Organics

(Cincinnati, OH). Decyl methacrylate (DMA) was purchased from Pfaltz and Bauer (Waterbury, CT). Tris(hydroxymethyl)aminomethane (Tris), ultrapure, molecular biology grade, was obtained from Research Organics (Cleveland, OH). Potassium phosphate monobasic and toluene were purchased from Mallinckrodt (Paris, KY). The [9]mercuracarborand-3 ionophore was synthesized as described previously.¹⁹ All aqueous solutions were prepared with 18 M Ω deionized reverse-osmosis water obtained by a Milli-Q water purification system (Millipore, Bedford, MA). Glass slides used in the experiment were obtained from Gold Seal Products (Portsmouth, NH). Glass coverslips were purchased from VWR (West Chester, PA). A polydimethylsiloxane (PDMS) Sylgard 184 elastomer kit (Dow Corning Corporation, Midland, MI) was used to fabricate the PDMS microfluidic discs used in the experiments. Polypropylene micropipet tips were purchased from Fisher Scientific (Cincinnati, OH). Seachem's Cichlid Lake Salt (Seachem Laboratories, Madison, GA) was donated by Just Fish in Lexington, KY.

Silanization of Glass Slides and Glass Coverslips. An 80% (v/v) solution of MPTS/toluene was made and placed in an evaporating dish. The glass slides, glass coverslips, and the evaporating dish were placed inside a vacuum desiccator. After 1.5 h, the vacuum was turned off and the slides and coverslips were left inside the desiccator for another 2 h.

Design and Fabrication of Microfluidic Disc. The structure was drawn and arrayed on a 120 mm diameter compact disc-shaped template in AutoCAD 2005 (Autodesk, San Rafael, CA) (one structure illustrated in Figure 1A). The detection chamber was 1.5 mm wide and 6 mm long and could hold 1.8 μ L. The solution reservoirs and the waste container were designed to contain 4.1 μ L and 20.5 μ L, respectively. The design was sent to CAD/Art Services (Bandon, OR), where a high-resolution proof was made on a transparency. The proof was then used to fabricate a master silicon wafer by conventional photolithography.

Preparation of PDMS. The Sylgard 184 elastomer kit contains a curing agent and silicone elastomer. A 1:10 ratio of curing agent to silicone elastomer was prepared and degassed under vacuum for 40 min. The gel was poured onto the silicon wafer mold and placed in an oven at 100 °C for 1 h. After curing, the PDMS disc was cut from the mold and removed. The depth of all reservoirs and microchannels was 200 μ m.

Preparation of Optode Membranes. All membrane cocktails were prepared with the following composition: 100 mg of DOS, 98 mg of HDDMA, 32 mg of DMA, 5.0 mg of benzoyl peroxide, and 2.5 mg of benzophenone. The solution was vortexed to dissolve the components. For the potassium optodes, 100 mg of cocktail, 1.9 mg of valinomycin (1.7×10^{-6} mol), and 1.5 mg of KTFPB (1.7×10^{-6} mol) were added and sonicated for 1 h to dissolve. Finally, 1.0 mg of chromoionophore III (1.7×10^{-6} mol) was added and vortexed to dissolve. All other optode membranes were prepared in the same manner. Different optode compositions were evaluated as described in the Results and Discussion section. The optimized membrane compositions contained 100 mg of cocktail in addition to the following components: sodium optodes, 3.5 mg of sodium ionophore X, 1.7 mg of NaTFPB, and 0.50 mg of chromoionophore III; chloride optodes, 5.5 mg of [9]mercura-

(14) Zoval, J. V.; Madou, M. J. *Proc. IEEE* **2004**, *92*, 140–153.

(15) Duffy, D. C.; Gillis, H. L.; Lin, J.; Sheppard, N. F.; Kellogg, G. J. *Anal. Chem.* **1999**, *71*, 4669–4678.

(16) Madou, M. J.; Kellogg, G. J. *Proc. SPIE-Int. Soc. Opt. Eng.* **1998**, *3259*, 80–93.

(17) Johnson, R. D.; Badr, I. H. A.; Barrett, G.; Lai, S.; Lu, Y.; Madou, M. J.; Bachas, L. G. *Anal. Chem.* **2001**, *73*, 3940–3946.

(18) Badr, I. H. A.; Johnson, R. D.; Madou, M. J.; Bachas, L. G. *Anal. Chem.* **2002**, *74*, 5569–5575.

(19) Yang, X.; Zheng, Z.; Knobler, C. B.; Hawthorne, M. F. *J. Am. Chem. Soc.* **1993**, *115*, 193–195.

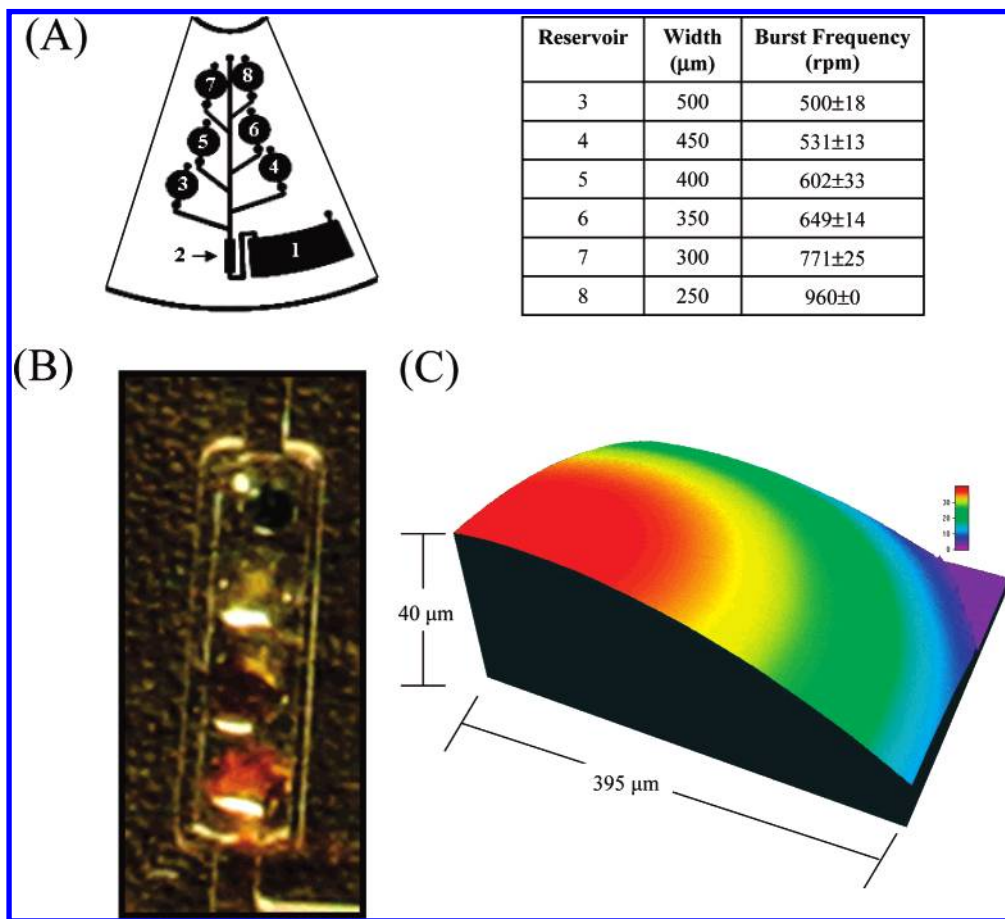


Figure 1. (A) AutoCAD drawing of a microfluidic structure on the CD. Features on the disc include a waste chamber (1), detection chamber (2), and solution reservoirs (3–8). The solution reservoirs are designed to release, sequentially, with the one furthest from the center (reservoir 3) releasing first. Inset table illustrates the widths of the microchannels connecting the circular reservoirs and the burst valves, as well as burst frequencies ($n = 3$) for each solution reservoir on the microfluidic disc; (B) Photograph of the microfluidic disc showing the four microdome optode array in the detection chamber; and (C) spatial representation of one-quarter of the optode microdome.

carborand-3, 3.0 mg of TDMAC, and 1.0 mg of chromoionophore VI; calcium optodes, 2.7 mg of calcium ionophore II, 1.5 mg of NaTFPB, and 1.0 mg of chromoionophore III. Optode membranes were spotted onto silanized glass slides and silanized glass coverslips using a polypropylene tip (inner diameter of 0.4 mm). A micropipet was not used to deliver a fixed volume of cocktail; the optode membranes were delivered via capillary action from the polypropylene tip to the surface. The microspots were simultaneously photopolymerized and covalently attached to the silanized glass substrate using a 100 W ultraviolet lamp at 366 nm (model B100AP Black-Ray, Upland, CA) in an oxygen-free environment for 8 min. One-quarter of this microdome optode is shown in Figure 1C. The image profile was acquired with a 10× objective via a NanoScale HS Optical Profiler System (Hyphenated-Systems, Burlingame, CA), which included a Nikon confocal microscope.

Preparation of Optode Microdome Array. Glass microscope coverslips were scored lengthwise with a diamond-tip glass cutter to a width of ~1.3 mm and then silanized in the manner previously described. Spotting of each optode membrane was performed, followed by photopolymerization. The section of the coverslip containing the microdomes was carefully removed along the score-line and then cut to a size of ~5.0 mm in length and placed inside the 1.5 mm × 6 mm detection chamber on the microfluidic disc

(shown in Figure 1B) with the unmodified coverslip surface facing the polycarbonate surface.

Calibration Measurements. Fluorescence measurements were taken using a Nikon Diaphot 200 microscope (Nikon Corporation, Melville, NY) with an attached photomultiplier tube (Electron Tubes Limited, United Kingdom). Details about the calibration procedure are provided in the Supporting Information. Briefly, the microdomes were first conditioned in 0.05 M Tris/ H_2SO_4 buffer, pH 7.4, for 30 min. For the initial experiments, six microdomes on a single silanized glass slide were chosen, and measurements were taken of the same six microdomes each time. These microdomes were equilibrated in a vial containing the appropriate KCl, NaCl, or CaCl_2 solution for 5 min, with a measurement taken after each equilibration. To obtain the fluorescence values for the fully protonated and deprotonated forms of the chromoionophore, measurements were taken after the microdomes were conditioned in vials of a $\text{KH}_2\text{PO}_4/\text{HCl}$ buffer (pH 2.9) and a 0.01 M NaOH solution, respectively, for 30 min.

Selectivity Measurements. To determine selectivity, the cation-selective optodes were conditioned in 1×10^{-5} , 1×10^{-3} , and 0.1 M solutions of LiCl, NaCl, KCl, CsCl, NH_4Cl , MgCl_2 , and CaCl_2 . For the chloride-selective optodes, conditioning was performed in 0.1 M solutions of Na_2SO_4 , NaBr, NaNO_3 , NaSCN, and sodium salicylate. All solutions were made in 0.05 M Tris/

H₂SO₄ buffer, pH 7.4. Calibrations for these ions were conducted in the same manner as described above.

Sample Concentration Determination. Water formulated to contain all of the ions found in Lake Tanganyika is used in aquaria for fish belonging to the family Cichlidae, commonly known as cichlids.²⁰ A sample of this water was prepared by dissolving 0.275 g of Seachem's Cichlid Lake Salt in 1 L of 0.05 M Tris/H₂SO₄ buffer, pH 7.4. Inductively coupled plasma (ICP) was employed for the determination of the concentrations of potassium, sodium, and calcium in the lake water, and ion chromatography was utilized for chloride concentration determination. The analyses with ICP and ion chromatography were performed at the Kentucky Geological Survey Laboratory of the University of Kentucky.

Centrifugal Microfluidics Disc Measurements. The six reservoirs contained the following solutions (Figure 1A): reservoir 3, 3×10^{-5} M KCl, 1×10^{-5} M NaCl, and 2×10^{-5} M CaCl₂; reservoir 4, 1×10^{-4} M KCl, 1×10^{-4} M NaCl, and 1×10^{-4} M CaCl₂; reservoir 5, 1×10^{-3} M KCl, 1×10^{-3} M NaCl, and 1×10^{-3} M CaCl₂; and reservoirs 6–8, real sample. Microdome optodes selective for potassium, sodium, calcium, and chloride were photopolymerized as an array onto single glass coverslips of 1.3 mm \times 5 mm in size. Conditioning of the microdomes in 0.05 M Tris/H₂SO₄ buffer, pH 7.4, was performed before placing the glass coverslips containing the microdomes in the detection chamber (denoted 2 in Figure 1A and shown in Figure 1B) on the microfluidic disc. Then, the cover disc was aligned with the solution delivery holes and a seal was formed between the cover and the PDMS disc. Calibrant and sample solutions were injected into the respective reservoirs. The instrumental system for the microfluidics experiments was divided into the following two sections: the control system and fluorescence excitation and detection. The control system has been described earlier.¹⁷ For fluorescence excitation and detection, the disc was slowed down to a stop, removed from the platform, and placed onto the stage of the Nikon Diaphot 200 microscope with an attached photomultiplier tube. Focusing was performed on a single microdome by blocking the fluorescence from the adjacent microdomes by using a mask, thus allowing only the fluorescence of the desired microdome to be observed. After the measurement was taken, the microfluidic disc was placed back on the platform and spun at the appropriate rate required to release the next solution.

RESULTS AND DISCUSSION

Theory. The sensing mechanism for the potassium, sodium, and calcium optodes is based on ion-exchange, where cations from the aqueous phase exchange with hydrogen ions inside the microdome. Response equations could be obtained for a given ionophore (L), lipophilic additive (R⁻), and chromoionophore (C) concentrations from generalized optode theory, as described by the following equation:^{21,22}

$$a_I = \left(\frac{1}{z_I K_{\text{ex}}^{\text{IL}}} \right) \left(\frac{\alpha}{1 - \alpha} a_H \right)^{z_I} \frac{R_T^- - (1 - \alpha) C_T}{\{L_T - (R_T^- - (1 - \alpha) C_T) (n_I/z_I)\}^{n_I}} \quad (1)$$

where a_I and a_H represent the activities of the primary ion and the hydrogen ion, respectively, z_I is the charge of the primary ion, $K_{\text{ex}}^{\text{IL}}$ is the exchange constant, α is the relative portion of deprotonated chromoionophore, n_I is the stoichiometry of the ion–ionophore complex, and R_T^- , C_T , and L_T are the total concentrations of the lipophilic additive, chromoionophore, and ionophore, respectively. The dynamic range could be adjusted, if needed for a particular application, by changing the pH or the relative amounts of the ionophore components in the membrane.²¹ The response of the chloride-selective microdome is based on the coextraction mechanism, i.e., chloride and hydrogen ions are simultaneously extracted into the membrane phase. The response is described by the following equation, where n_I could have a value of 1 or 2 depending on the ratio of the ion–ionophore complex (vide infra):²³

$$a_I a_H = \left(\frac{1}{z_I K_{\text{coex}}} \right) \left(\frac{1 - \alpha}{\alpha} \right) \frac{(1 - \alpha) C_T}{\{L_T - n_I (1 - \alpha) C_T\}^{n_I}} \quad (2)$$

The following equation was used to relate the measured fluorescence, F , at given activity a_I to α :²⁴

$$\alpha = \frac{F_P - F}{F_P - F_D} \quad (3)$$

where F_P and F_D are the fluorescence emission signals of the fully protonated and fully deprotonated forms of the chromoionophore, respectively.

To calculate the selectivity coefficient, K_{IJ}^{opt} , where I is the primary ion and J is the interfering, or secondary, ion at a chosen pH value, the following equation, which employs the separate solution method (SSM), can be used:^{21,25}

$$K_{IJ}^{\text{opt}} = \frac{a_I}{(a_J)^{z_I/z_J}} \quad (4)$$

where a_I and a_J are the activities of I and J, respectively, at a given degree of protonation of the chromoionophore. K_{IJ}^{opt} values can be used to compare optode selectivity to ISE selectivity coefficients.

Calibration and Selectivity. Calibrations were performed using microdomes applied on silanized glass slides. For each ion calibration, six microdomes were exposed sequentially to standard solutions of increasing ion concentration from 1×10^{-6} to 1.0 M in 0.05 M Tris/H₂SO₄, pH 7.4. To study the selectivity of the cation-selective optodes (potassium, sodium, and calcium), the signals at 1×10^{-5} , 1×10^{-3} , and 0.1 M LiCl, NaCl, KCl, NH₄Cl, CsCl, MgCl₂, and CaCl₂ were measured. To establish the selectivity of

(20) Oliver, M. K. The Cichlid Fishes of Lake Malawi, Africa. <http://malawicichlids.com/mw01011.htm> (accessed April 2007).

(21) Bakker, E.; Bühlmann, P.; Pretsch, E. *Chem. Rev.* **1997**, *97*, 3083–3132.

(22) Johnson, R. D.; Bachas, L. G. *Anal. Bioanal. Chem.* **2003**, *376*, 328–341.

(23) Ceresa, A.; Qin, Y.; Peper, S.; Bakker, E. *Anal. Chem.* **2003**, *75*, 133–140.

(24) Shortreed, M.; Bakker, E.; Kopelman, R. *Anal. Chem.* **1996**, *68*, 2656–2662.

(25) Bakker, E.; Simon, W. *Anal. Chem.* **1992**, *64*, 1805–1812.

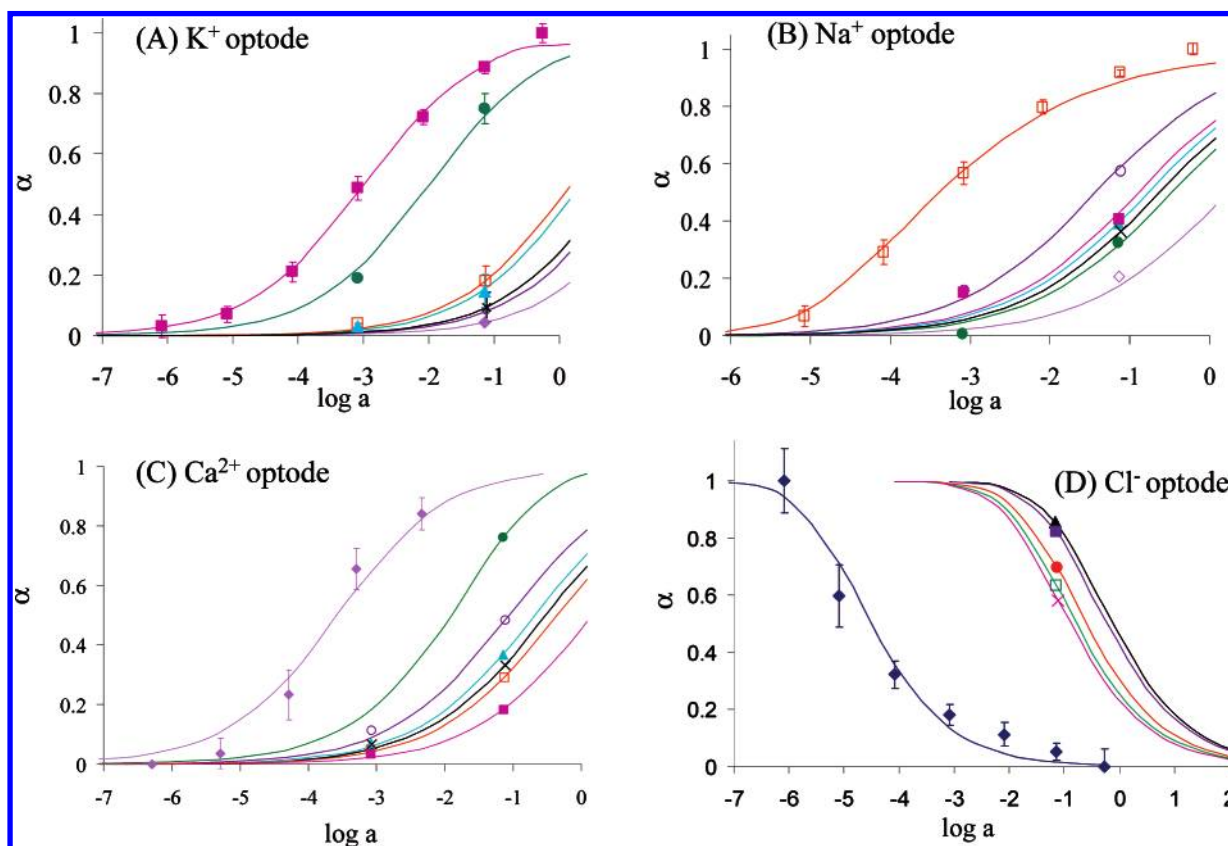


Figure 2. Calibration of primary and interfering ions for the microdome optodes in 0.05 M Tris/H₂SO₄ buffer, pH 7.4. Error bars represent one standard deviation ($n = 6$). For cation-selective microdomes (■) potassium, (●) cesium, (×) magnesium, (□) sodium, (▲) ammonium, (○) lithium, and (◆) calcium. (A) Potassium microdome optode. The solid line represents the theoretical response according to eq 1 for $n_1 = 1$ and $K_{\text{ex}}^{\text{K}^+/\text{L}} = 3.9 \times 10^{-5}$. (B) Sodium microdome optode. The solid line represents the theoretical response according to eq 1 for $n_1 = 2$ and $K_{\text{ex}}^{\text{Na}^+/\text{L}} = 1.4 \times 10^{-4}$. (C) Calcium microdome optode. The solid line represents the theoretical response according to eq 9 of Bakker et al.³⁸ for $K_{\text{ex}}^{\text{Ca}^{2+}/\text{L}} = 5.7 \times 10^{-8}$. (D) Chloride microdome optode response to (◆) chloride, (×) salicylate, (□) bromide, (●) thiocyanate, (■) nitrate, and (▲) sulfate. The solid line represents the theoretical response according to eq 2 for $n_1 = 1$ and $K_{\text{coex}} = 5.6 \times 10^{12}$.

the chloride-selective optodes, the signal obtained with 0.1 M Na₂SO₄, NaBr, NaNO₃, NaSCN, and sodium salicylate was recorded. After each measurement, a different set of six optodes on a silanized glass slide was used.

Potassium-selective microdome optodes containing the ionophore valinomycin and chromoionophore ETH 5350 have been characterized previously using a CCD camera as detector.²⁶ The response and selectivity parameters of these optodes were reevaluated employing a photomultiplier tube (PMT) for detection, which is more sensitive than the CCD camera used in the previous study. The calibration for potassium along with the theoretical response curve generated from eq 1 is illustrated in Figure 2A. The experimental results fit well with the theoretical response, illustrating that the ion-exchange mechanism of bulk optodes also governs the response of the microdomes. Additionally, the error at each concentration was reduced when utilizing the PMT for detection instead of the CCD. The dynamic range of the potassium optode membrane extends over ~3 decades of activity (from 2.0×10^{-5} to 6.3×10^{-2} M). The observed exchange constant, $K_{\text{ex}}^{\text{K}^+/\text{L}}$, calculated from the experimental points and eq 1 is 3.9×10^{-5} . Figure 2A also shows the theoretically predicted calibration curves based on the optode response function for sodium, lithium,

cesium, magnesium, and calcium. At constant pH, and at a given α , $K_{\text{K}^+/\text{J}}^{\text{opt}}$ can be obtained from eq 3.^{21,25} In each case described herein, $\alpha = 0.5$ was used to calculate the $\log K_{\text{K}^+/\text{J}}^{\text{opt}}$ values summarized in Table 1. The valinomycin-based sensing microdomes displayed selectivities comparable to those found in optodes based on other polymer matrixes,^{27–29} as well as those incorporating BME-44 as the potassium ionophore in a PVC–DOS matrix.³⁰

Sodium ionophore X, a calix[4]arene tetraester, was used to prepare sodium-sensing microdomes, which also employ ETH 5350 as the chromoionophore. Different ratios of L:R:C were evaluated to determine the optimum membrane composition. First, membranes containing ratios of 1:1:1 and 2:1:1 were tested, but neither displayed an appropriate response to sodium at pH 7.4. Better results were obtained with a 4:2:1 ratio. However, when theoretical fitting was performed on the experimental data, the data did not fit well with the theoretical response function corresponding to a 1:1 ion–ionophore complex (eq 1), as shown by the dashed line in Figure 3. Rather, the data fit better a 1:2 ion–ionophore complex stoichiometry (--- in Figure 3). It has

(26) Watts, A. S.; Urbas, A. A.; Finley, T.; Gavalas, V. G.; Bachas, L. G. *Anal. Chem.* **2006**, *78*, 524–529.

(27) Ambrose, T. M.; Meyerhoff, M. E. *Anal. Chim. Acta* **1999**, *378*, 119–126.

(28) Wang, E.; Zhu, L.; Ma, L.; Patel, H. *Anal. Chim. Acta* **1997**, *357*, 85–90.

(29) Suzuki, K.; Ohzora, H.; Tohda, K.; Miyazaki, K.; Watanabe, K.; Inoue, H.; Shirai, T. *Anal. Chim. Acta* **1990**, *237*, 155–164.

(30) Wygladacz, K.; Bakker, E. *Anal. Chim. Acta* **2005**, *532*, 61–69.

Table 1. Selectivity Coefficients, $\log K_{IJ}^{\text{opt}}$, for Ion-Selective Microspotted Optodes at pH 7.4, Calculated by the Separate Solutions Method

cation	$\log K_{K+J}^{\text{opt}}$	$\log K_{Na+J}^{\text{opt}}$	$\log K_{Ca^{2+}+J}^{\text{opt}}$
K ⁺	0	-2.49	-3.90
Cs ⁺	-1.00	-2.91	-0.73
Na ⁺	-3.17	0	-2.89
NH ₄ ⁺	-3.33	-2.61	-2.23
Mg ²⁺	-3.41	-2.75	-3.08
Ca ²⁺	-3.75	-3.60	0
Li ⁺	-4.00	-1.96	-1.49

anion	$\log K_{Cl-J}^{\text{opt}}$
Cl ⁻	0
salicylate	-3.80
Br ⁻	-3.91
SCN ⁻	-4.09
SO ₄ ²⁻	-4.63
NO ₃ ⁻	-4.48

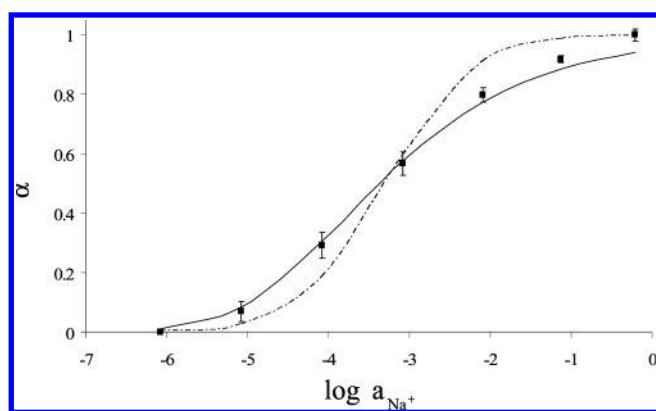


Figure 3. Sodium microdome optode calibration with theoretical fittings for 1:1 and 1:2 ion–ionophore complexes. Experimental data are shown as ■. The solid line represents the fitting for a 1:2 complex and the dashed line represents the theoretical response for a 1:1 complex.

been shown previously that this calix[4]arene,³¹ as well as other similar calix[4]arenes,³² can form 1:2 ion–ionophore complexes, in addition to 1:1 complexes. Alternatively, it is possible that the photopolymerization reaction generates variants of the ionophore leading to a response that deviates from that expected from the more common 1:1 stoichiometry. The calibration curves for sodium along with responses to potentially interfering cations are shown in Figure 2B. The dynamic range extends over ~2 decades of activity (from (1×10^{-5}) to (2.5×10^{-3}) M). An exchange constant, $K_{\text{ex}}^{\text{Na}^+\text{L}}$, of 1.4×10^{-4} for Na⁺ was observed for this system. The sodium-sensing microspotted optodes displayed good selectivity coefficients for sodium against all other interfering cations evaluated (Table 1). In another system employing the same ionophore, but a different polymer matrix and chromoionophore in a spin-coated membrane configuration, comparable selectivity coefficients for potassium and calcium, two of the potential interferents for the system described herein, were obtained.³³ In

addition to selectivity coefficients, selectivity factors, k_{IJ}^{Osel} , are used to describe the selectivity of optodes (eq 5):²¹

$$K_{IJ}^{\text{opt}} = (k_{IJ}^{\text{Osel}})^{z_I/z_J} a_I(I)^{1-(z_I/z_J)} \quad (5)$$

where $a_I(I)$ is the primary ion activity in the sample in the absence of interfering ions. Comparable selectivity factors, k_{Na+J}^{Osel} , for the optode microdomes and PVC-based microsphere optodes employing sodium ionophore X as the sensing element were also observed.^{30,34}

As with the potassium and sodium-sensing microdomes, the calcium-sensing microdomes also incorporated ETH 5350 as the chromoionophore. The ionophore employed in this system was ETH 129, or calcium ionophore II. Previous calcium-sensing PVC microspheres have been prepared with an acrylic derivative of this ionophore (AU-1), which was covalently attached to a methyl methacrylate–dodecyl methacrylate polymer matrix, in order to make the sensors more amenable for sensing in the physiological concentration range.³⁵ ETH 129 has been shown to form 1:1, 1:2, and 1:3 ion–ionophore complexes,³⁶ with 1:3 complexes being the most common.³⁷ As the concentration of calcium increases, the prevalence of the 1:1 and 1:2 ion–ionophore complexes, increases.³⁶ In the microdome optode system described herein, the theoretical equation describing a 1:3 ion–ionophore complex did not fit the experimental data, which could be explained by the presence of complexes of other stoichiometries. Modeling equations of optode response for mixtures of different ion–ionophore stoichiometries have been described earlier.³⁸ Fitting the experimental data to different ion–ionophore stoichiometries was examined using these modeling equations, and it was determined that the response of the calcium-sensing microdomes can be described by a mixture of 1:2 and 1:3 ion–ionophore complexes. The apparent exchange constant, $K_{\text{ex}}^{\text{Ca}^{2+}\text{L}}$, for the calcium-sensing microdomes was found to be 5.7×10^{-8} . An acceptable measuring range $((1.6 \times 10^{-5}) - (1 \times 10^{-2})$ M) was observed as seen in Figure 2C, as well as good selectivities over common interfering cations (Table 1). Selectivities comparable to PVC-based optical microspheres with AU-1^{30,34} were obtained with these sensing microdomes.

While the response mechanism for the potassium-, sodium-, and calcium-sensing microdomes is based on ion-exchange, the chloride-selective microdome response is governed by coextraction. In this system, chloride and hydrogen ions are simultaneously extracted into the membrane phase. Upon the selective binding of chloride by the [9]mercuracarborand-3 ionophore, H⁺ must be coextracted to protonate the acidic chromoionophore to maintain electroneutrality inside the membrane. As the chloride concentration increases, the extent of proton coextraction increases, resulting in an increase in the extent of protonation of

(31) Israëli, Y.; Detellier, C. *J. Phys. Chem. B* **1997**, *101*, 1897–1901.

(32) Baklouti, L.; Abidi, R.; Vicens, J.; Asfari, Z.; Harrowfield, J.; Rokbani, R. *J. Inclusion Phenom. Mol. Recognit. Chem.* **2002**, *42*, 197–201.

(33) Yang, X.; Wang, K.; Xiao, D.; Guo, C.; Xu, Y. *Talanta* **2000**, *52*, 1033–1039.

(34) Xu, C.; Wygladacz, K.; Qin, Y.; Retter, R.; Bell, M.; Bakker, E. *Anal. Chim. Acta* **2005**, *537*, 135–143.

(35) Qin, Y.; Peper, S.; Radu, A.; Ceresa, A.; Bakker, E. *Anal. Chem.* **2003**, *75*, 3038–3045.

(36) Wang, E.; Erdahl, W. L.; Hamidinia, S. A.; Chapman, C. J.; Taylor, R. W.; Pfeiffer, D. R. *Biophys. J.* **2001**, *81*, 3275–3284.

(37) Schefer, U.; Ammann, D.; Pretsch, E.; Oesch, U.; Simon, W. *Anal. Chem.* **1986**, *58*, 2282–2285.

(38) Bakker, E.; Willer, M.; Lerchi, M.; Seiler, K.; Pretsch, E. *Anal. Chem.* **1994**, *66*, 516–521.

the acidic chromoionophore, as well. Thus, when monitoring the basic form, a decrease in fluorescence is observed with increasing chloride concentration. Previous spin-coated optode membranes prepared with [9]mercuracarborand-3 and containing PVC as the polymer matrix and 2-nitrophenyl octyl ether as the plasticizer were based on a 2:1:1 (L/R/C) ratio.³⁹ However, when this composition was evaluated using the DMA–HDDMA polymer matrix, an acceptable calibration curve was not obtained. This result prompted us to evaluate additional compositions, which included 4:1:1 and 4:2:1 (L/R/C) ratios. Microdomes prepared with these ratios resulted in optodes that did not display a response that agreed with the one described by eq 2. A possible explanation is that residual negative charges from the methacrylate are present inside the microdomes, necessitating additional cationic sites to counterbalance this effect. If an excess of cationic sites were not incorporated into the microdomes, the residual negative charges would lessen the extent of chloride extraction into the microdome, thus lessening the extent of proton coextraction and distorting the optode response. Additional MC3-containing microdomes were prepared with 4:4:1 and 6:6:1 compositions, and it was determined that a 4:4:1 L/R/C ratio gave the best results.

In addition to forming 1:1 complexes with chloride, Bakker and co-workers have shown that [9]mercuracarborand-3 forms 2:1 ionophore–ion complexes in PVC–DOS films.²³ Theoretical fittings based on both 1:1 and 2:1 ionophore–ion complexes were performed. On the basis of these theoretical fittings, 1:1 complexes must be favored in the DMA–HDDMA matrix. This result is consistent with the finding by Bakker and co-workers that found that in order to exclusively form 1:1 complexes, at least 50 mol % of additive relative to the ionophore is needed.²³ In the case described herein, equimolar amounts of [9]mercuracarborand-3 and TDMAC were incorporated into the cocktail. The response for chloride and those for sulfate, bromide, nitrate, thiocyanate, and salicylate are shown in Figure 2D. As seen from the figure and from the selectivity coefficients in Table 1, very good selectivity for chloride over other potentially interfering anions was obtained with the 4:4:1 L/R/C ratio of membrane components at pH 7.4. Since this is the first chloride optode based on [9]mercuracarborand-3 that employs decyl methacrylate as the polymer matrix, comparisons of the selectivity coefficients were made to thin film systems composed of either PVC–NPOE³⁹ or PVC–DOS.⁴⁰ The calculated selectivity coefficients, in most cases, demonstrated an improvement in the selectivity for all ions examined.^{39,40}

Microdome Arrays. Different types of microarrays have been fabricated by methods such as ink-jet printing or microspotting, which directly spot the molecules of interest onto a substrate.⁴¹ The technique of microspotting has been an effective method of microfabricating protein, DNA, and carbohydrate arrays.^{42–48} With the use of these methods, the simultaneous (i.e., in parallel)

delivery of uniform volumes/amounts of sensing elements to a surface is possible. The sensing microdome systems described herein could be microfabricated using this method, producing an array of microdomes capable of sensing potassium, sodium, calcium, and chloride.

In order to employ each of these microspotted optodes in an array to simultaneously sense for potassium, sodium, calcium, and chloride within a μ TAS network, calibration of each of the optodes must ideally be accomplished with a solution containing all of the ions with minimal cross-interference. This should reduce the number of calibrant solutions needed and greatly simplify the operation of the μ TAS. The mixed ion calibrant solutions were designed so that the response from potential interfering ions is minimal. The following solutions were chosen as calibrants: Calibrant I, 3.0×10^{-5} M KCl, 1.0×10^{-5} M NaCl, and 2.0×10^{-5} M CaCl₂; Calibrant II, 1.0×10^{-4} M KCl, 1.0×10^{-4} M NaCl, 1.0×10^{-4} M CaCl₂; and Calibrant III, 1.0×10^{-3} M KCl, 1.0×10^{-3} M NaCl, and 1.0×10^{-3} M CaCl₂. This resulted in chloride concentrations of 8.0×10^{-5} M, 4.0×10^{-4} M, and 4.0×10^{-3} M in Calibrant I, II, and III, respectively.

The following equation, based on optode theory, was used to calculate the extended response function for the cation-selective optode microdomes in a sample containing interfering ions (J^+):²¹

$$a_I + k_{IJ}^{\text{Osel}} a_J = (z_I K_{\text{ex}}^{\text{IL}})^{-1} \left(\frac{\alpha}{1 - \alpha} a_H \right)^{z_I} \frac{R_T - (1 - \alpha) C_T}{\{L_T - (R_T - (1 - \alpha) C_T) n_I / z_I\}^{n_I}} \quad (6)$$

By employment of the concentrations chosen for Calibrants I, II, and III, the error induced by the simultaneous calibration of the microdome optodes with solutions containing all of the ions is calculated to be less than 1.3% in all cases. Thus, it is feasible to calibrate all four microdomes with the same three calibrant solutions without introducing a significant error in the measurement due to ion interference in the calibration.

Integration of Optode Microdomes with Centrifugal Microfluidics. Centrifugal microfluidics platforms operate on the basis of radial forces developed from spinning the CD in conjunction with passive capillary valves that create fluid flow discontinuity. These valves are constructed after each reservoir on the platform by adjusting the diameter of the channels connected to the reservoirs. When the angular frequency increases beyond a set frequency, the “burst frequency”, the radial forces overcome the surface tension at the “burst” valve and fluid flows from the reservoir to the detection chamber. The reservoirs on the centrifugal microfluidics platform were designed so that the solutions contained in them would release sequentially and separately beginning with reservoir 3. The burst frequencies for each of the circular solution reservoirs (Figure 1A) were tested to ensure adequate spacing in terms of rpm of the fluid release from each structure. All channel depths were 200 μ m, and the

(39) Badr, I. H. A.; Johnson, R. D.; Diaz, M.; Hawthorne, M. F.; Bachas, L. G. *Anal. Chem.* **2000**, *72*, 4249–4254.

(40) Xu, C.; Qin, Y.; Bakker, E. *Talanta* **2004**, *63*, 180–184.

(41) Venkatasubbarao, S. *Trends Biotechnol.* **2004**, *22*, 630–637.

(42) Cho, E. J.; Tao, Z.; Tehan, E. C.; Bright, F. V. *Anal. Chem.* **2002**, *74*, 6177–6184.

(43) Shumaker-Parry, J. S.; Zareie, M. H.; Aebbersold, R.; Campbell, C. T. *Anal. Chem.* **2004**, *76*, 918–929.

(44) MacBeath, G.; Schreiber, S. L. *Science* **2000**, *289*, 1760–1763.

(45) Lee, K.; Park, S.; Mirkin, C. A.; Smith, J. C.; Mrksich, M. *Science* **2002**, *295*, 1702–1705.

(46) Ito, Y.; Nogawa, M. *Biomaterials* **2003**, *24*, 3021–3026.

(47) Delehanty, J. B.; Ligler, F. S. *Anal. Chem.* **2002**, *74*, 5681–5687.

(48) Carroll, G. T.; Wang, D.; Turro, N. J.; Koberstein, J. T. *Langmuir* **2006**, *22*, 2899–2905.

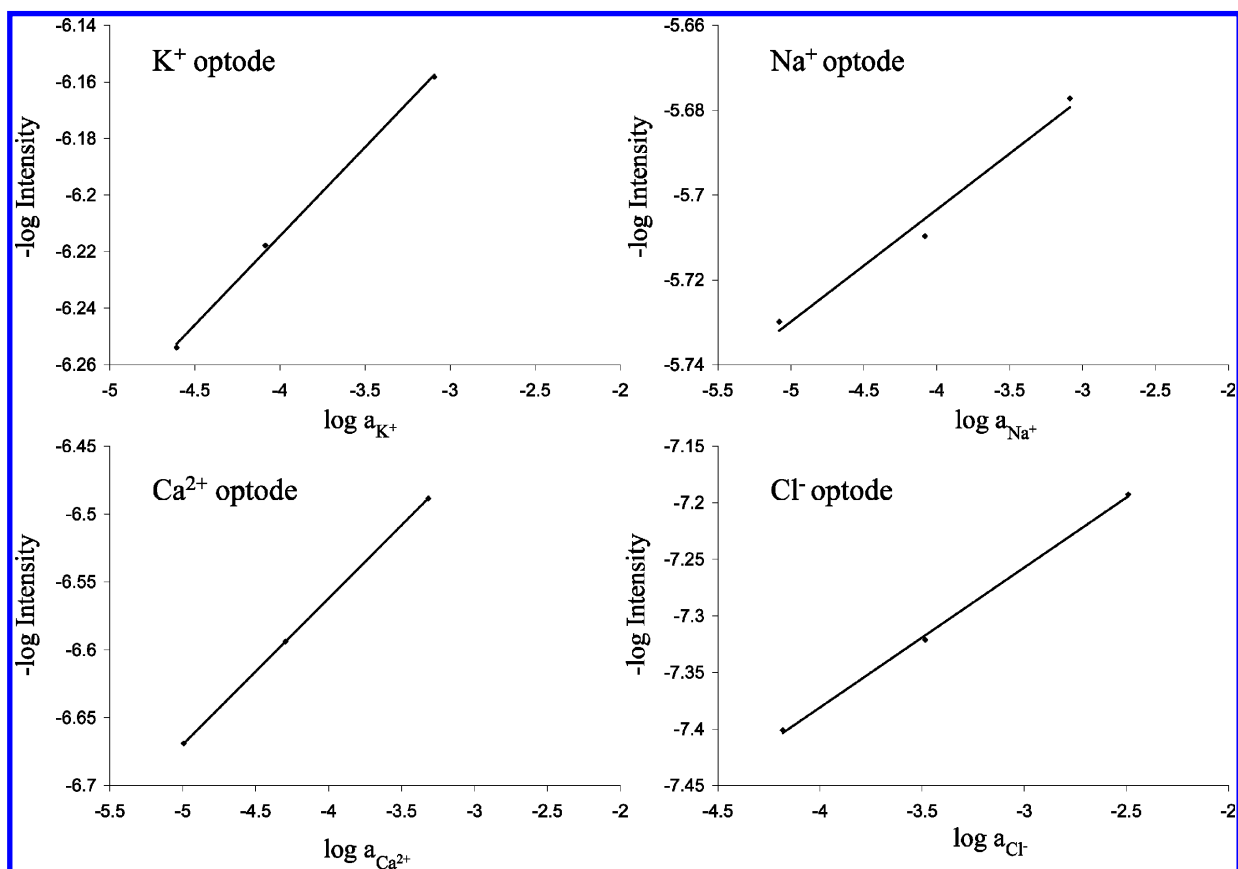


Figure 4. Simultaneous calibration of the four microdome optodes using three calibrant solutions: 3.0×10^{-5} M KCl, 1.0×10^{-5} M NaCl, and 2.0×10^{-5} M CaCl_2 (Calibrant I); 1.0×10^{-4} M KCl, 1.0×10^{-4} M NaCl, 1.0×10^{-4} M CaCl_2 (Calibrant II); and 1.0×10^{-3} M KCl, 1.0×10^{-3} M NaCl, and 1.0×10^{-3} M CaCl_2 (Calibrant III).

widths of the channels connecting the solution reservoirs and the burst valves for reservoirs 3, 4, 5, 6, 7, and 8 (Figure 1A) were 500, 450, 400, 350, 300, and 250 μm , respectively. To determine the angular frequency required for the solutions to be released from the reservoirs (i.e., the burst frequency), each reservoir was filled with a differently colored solution. The angular frequency was increased stepwise until the release of the solution from the appropriate reservoir. The results are shown in the inset table in Figure 1 and demonstrate that each reservoir would release without the subsequent reservoir releasing simultaneously.

The centrifugal microfluidics disc described herein was designed to be amenable to various combinations of calibrants and samples. Different procedures in calibration of the microdomes and analysis of samples were evaluated for their efficiency. The goal of this system was to employ the minimal number of calibrant solutions required in order to accurately determine the concentration of potassium, sodium, calcium, and chloride in a sample containing these ions. While many commercial systems, including the i-STAT system described previously, rely on one-point calibrations, this scenario was not evaluated. By employment of a two- or three-point calibration with solutions whose concentrations fall within the working range of the response, the accuracy of the analysis is improved substantially. Attempts to calibrate the microdome optode array with only two standard solutions and to analyze a real sample resulted in unacceptable errors for the concentrations of each ion determined from the theoretical response curves. The reason for this error arises from errors in

the measurement of the calibrant solutions, and is translated to the entire response curve. Since it has been demonstrated that ion-selective optodes can be calibrated based on the linear range of the theoretical response,^{17,18} this method was explored in the system described here and will be discussed later.

Potassium-, sodium-, calcium-, and chloride-sensing optodes were microspotted in an array onto a silanized glass microscope coverslip of ~ 1.3 mm in width. After photopolymerization, these coverslips were cut to fit inside the detection chamber on the microfluidic disc and were conditioned in 0.05 M Tris/ H_2SO_4 buffer, pH 7.4, prior to use. The polycarbonate cover was then placed over the PDMS disc containing the optode array, forming a seal. Calibrant solutions were dispensed into reservoirs 3–5. Reservoir 3 was filled with Calibrant I, reservoir 4 with Calibrant II, and reservoir 5 with Calibrant III. Reservoirs 6–8 contained a sample of aquarium water (a Lake Tanganyika water simulant) prepared from Seachem's Cichlid Lake Salt dissolved in 0.05 M Tris/ H_2SO_4 , pH 7.4, buffer. The microfluidic disc was rotated at the frequency required to release the solution from the appropriate reservoir and then stopped after the solution reached the detection chamber. After the microdomes were conditioned for the appropriate time period, the microfluidic disc was removed from the platform and placed onto the stage of the epifluorescence microscope. When the fluorescence measurement on one particular microdome was performed, a mask with a 1 mm hole was placed over the detection chamber to allow fluorescence to be recorded from a single microdome without interference from the other three microdomes. After fluorescence measurements were taken of each

Table 2. Concentrations of Potassium, Sodium, and Calcium Determined by ICP and Chloride Determined by Ion Chromatography in Comparison to the Concentrations Found Employing the Microfluidic System for Three Aquarium Water Samples (Simulating Lake Tanganyika Water)^a

ion	concentration (M)		% error
	ICP or IC	centrifugal microfluidic system	
potassium	$4.42 (\pm 0.01) \times 10^{-4}$	$4.67 (\pm 0.24) \times 10^{-4}$	5.6
sodium	$3.56 (\pm 0.01) \times 10^{-4}$	$3.38 (\pm 0.34) \times 10^{-4}$	5.0
calcium	$1.35 (\pm 0.004) \times 10^{-4}$	$1.38 (\pm 0.12) \times 10^{-4}$	1.9
chloride	7.21×10^{-4}	$7.44 (\pm 0.58) \times 10^{-4}$	3.2

^a The average \pm standard deviation ($n = 3$) is reported, along with the percent error in the measurement.

microdome, the disc was placed back onto the platform and rotated at the frequency required to release the solution from the next reservoir. This procedure was repeated until measurements had been taken from all solutions.

In conventional optodes, experimental data are fitted to the theoretical response function of eq 1 by converting the optical signal to the response parameter, α (eq 3). Calculation of α values requires that the signal corresponding to fully protonated and fully deprotonated chromoionophore be obtained. As shown earlier, fitting of the data to a response function was used to obtain information about the ion–ionophore complexation stoichiometries. However, knowledge of α values is not necessary to calibrate the optodes. With the choice of calibration standards with concentrations within the linear response range for each optode, the logarithm of fluorescence signal intensity can be plotted versus the logarithm of activity of each ion to obtain a calibration plot.¹⁷ Triplicate analysis of the same sample or analysis of three different samples can be performed within a single microfluidic network on the CD. To illustrate this feature, three aliquots of the same aquarium water sample were delivered to reservoirs 6–8. The linear calibration plots obtained from the three mixed ion standard solutions are illustrated in Figure 4 and were used to determine the concentration of the ions of interest in the aquarium water sample. Very good precision was observed for the fluorescence intensity values for the three sample solutions with all of the microdome optodes (less than 1% RSD in the fluorescence intensity). Table 2 displays the concentrations of the ions in the aquarium water sample determined by ICP or ion chromatography and the concentrations found using the centrifugal microfluidics platform. As seen from the table, errors of less than 6% were observed for all analyses. Whereas a 1.3% error was calculated earlier for the simultaneous calibration method, the actual error found was greater and can be attributed to overall method error. At 95% confidence, the values from the two analytical methods (CD vs ICP or ion chromatography) are the same. These results demonstrate the feasibility of employing this microfluidic system for the accurate determination of the con-

centration of potassium, sodium, calcium, and chloride in the aquarium water. Further, an inherent advantage in this integrated system is the sequential calibration of the microdome optodes using mixed ion calibrant solutions and the quantification of ion concentration(s) in a sample. Since in each microfluidic network, the sample is paired with its own set of calibrants, the analysis of a sample is not affected by the day-to-day variations in the environmental conditions, or other parameters that may affect the signal of the microdomes (for example, storage period).

CONCLUSIONS

The microdome optode array incorporated into the centrifugal microfluidic system discussed in this article presents an attractive method for the simultaneous analysis of various ions in complex samples. Decyl methacrylate-based potassium-, sodium-, calcium-, and chloride-sensing microspotted optodes were developed to incorporate into this array. Whereas other systems rely on one-point calibration, three-point calibration is possible using this microfluidic platform. Calibration was performed with three mixed-ion standard solutions containing all of the necessary ions without significant interference from other ions in the calibrant solutions. Good agreement with the theoretical response for each sensing optode was observed. These microdomes were evaluated using an aquarium water sample. The concentrations of all four ions were determined simultaneously using the microdome array with <6% error for the real water sample. In addition, the manner in which the microdome arrays are fabricated makes them amenable to mass production, increasing the feasibility for commercial use. This system could be extended for other applications by simply changing the pH and/or the ratios of the membrane components in order to shift the measuring range for the four ions into that required for a particular application. It should be noted that the centrifugal microfluidics system could be integrated with fiber optics-based detection to further automate the analysis. The software employed to control the stepper motor is capable of decelerating the disc to a stop at precise positions so that each of the detection chambers could be aligned sequentially with stationary fiber optics to facilitate measurements from individual microdomes. This integration should result in the development of portable multiion detection systems.

ACKNOWLEDGMENT

The authors thank the National Aeronautics and Space Administration and the Kentucky Research Challenge Trust Fund for financial support.

SUPPORTING INFORMATION AVAILABLE

Additional information as noted in text. This material is available free of charge via the Internet at <http://pubs.acs.org>.

Received for review May 3, 2007. Accepted August 9, 2007.

AC0709100